Journal of Cellular Plastics

http://cel.sagepub.com

Engineering of Foamed Structures for Biomedical Application

A. Salerno, P.A. Netti, E. Di Maio and S. Iannace

Journal of Cellular Plastics 2009; 45; 103
DOI: 10.1177/0021955X08099929

The online version of this article can be found at:
http://cel.sagepub.com/cgi/content/abstract/45/2/103

Published by:
SAGE
http://www.sagepublications.com

Additional services and information for *Journal of Cellular Plastics* can be found at:

Email Alerts: http://cel.sagepub.com/cgi/alerts

Subscriptions: http://cel.sagepub.com/subscriptions

Reprints: http://www.sagepub.com/journalsReprints.nav

Permissions: http://www.sagepub.co.uk/journalsPermissions.nav

Citations http://cel.sagepub.com/cgi/content/refs/45/2/103

Downloaded from http://cel.sagepub.com at Matematica Applicata E on February 19, 2009

Engineering of Foamed Structures for Biomedical Application

A. SALERNO AND P. A. NETTI*
Interdisciplinary Research Centre on Biomaterials (CRIB) and Italian Institute of Technology (IIT), Piazzale Tecchio 80, 80125 Naples, Italy

E. DI MAIO
Department of Materials and Production Engineering, University of Naples Federico II, P.le Tecchio 80, 80125 Naples, Italy

S. IANNACE
Institute of Composite and Biomedical Materials, National Research Council (IMCB-CNR), Piazzale Tecchio 80, 80125, Naples, Italy

ABSTRACT: The aim of this study was to combine gas foaming (GF) and reverse templating techniques to prepare open-pore polymeric foams with pore structures specifically designed for tissue engineering. Poly(ε-caprolactone) (PCL) has been melt mixed with two different templating agents, NaCl microparticles and thermoplastic gelatin (TG), to prepare microparticulate composites and co-continuous blends, respectively. These heterogeneous systems have been subsequently gas foamed by using mixtures of N_2 and CO_2 as blowing agents. Finally, the foamed materials have been soaked in H_2O to selectively extract the NaCl or TG from the polymeric matrices to achieve the final foamed structure. The presence of the different templating agents extensively affected the foaming process of PCL; these effects have been analyzed and the results gathered important information to design porous scaffolds with fine tuned open-pore architectures. In particular, the control of the overall porosity, pore size and shape, pore interconnectivity, and spatial distribution of PCL matrix has been achieved by optimizing the GF process parameters with respect to the specific templating system. Results demonstrated that the combination of the GF and reverse templating techniques allowed the preparation of PCL scaffolds with open-pore architectures and highly controlled porosity and pore size spatial distribution.

*Author to whom correspondence should be addressed. E-mail: nettipa@unina.it

0021-955X/09/02 0103–16 $10.00/0 DOI: 10.1177/0021955X08099929
© SAGE Publications 2009
Los Angeles, London, New Delhi and Singapore

Downloaded from http://cel.sagepub.com at Matematica Applicata E on February 19, 2009

KEY WORDS: gas foaming, poly(ε-caprolactone), reverse templating, scaffold, tissue engineering.

INTRODUCTION

Tissue engineering (TE) is an interdisciplinary science involving the basic principles of engineering and life science, and its ultimate challenge is the regeneration of biological substitutes for damaged tissues and organs. One of the most promising approach developed in TE is the design of biocompatible and biodegradable porous scaffolds able to guide transplanted cells during new-tissue regeneration [1]. Three-dimensional biodegrading scaffolds act as temporary substitute for the extracellular matrix, promoting cell adhesion, proliferation and migration, and sustaining the mechanical load until the regeneration process is completed [2].

From the point of view of the scaffold design, a large number of studies showed that not only the physicochemical properties of the polymeric matrix, but also the architecture of the porous structure of the scaffold control cell seeding, migration and biosynthesis, and consequently, affect the functionalities of the new tissue. In particular, the overall porosity, the pore size and interconnectivity and the porosity and pore size spatial distribution are key microstructural issues in biomedical applications [3–6].

The overall porosity of the scaffold is somehow related to its surface-to-volume ratio that define the surface available for cell attachment, and consequently, large porosities are preferable for the regeneration of tissues characterized by a high cell density [7]. As a matter of fact, for load-bearing application, such as bone and cartilage repair, there may be a conflict between maximizing cell density and optimizing the mechanical response of the scaffold. This aspect often leads to a compromise in the design of the scaffold properties [8].

The regeneration of specific tissues has been shown to be strongly dependent also on the pore size of the supporting 3D structure that has to allow the in-growth of specific cell type [4,7]. In particular, *in vitro* and *in vivo* experimental tests demonstrated that, in the case of neo-vascularization, optimal pore size is 5 μm, while 5–15 μm pore size is suitable for fibroblast in-growth, 20–125 μm for regeneration of adult mammalian skin, 100–350 μm for regeneration of bone, and >500 μm for rapid vascularization [3].

Pore interconnectivity within the scaffold is also an essential design parameter in tissue regeneration processes. In fact, material transport and cell migration would be inhibited if the pores are not well interconnected, even if the porosity of the matrix is high [5].

Downloaded from http://cel.sagepub.com at Matematica Applicata E on February 19, 2009

The architecture of the porous structure may be designed through the proper selection of the fabrication techniques and processing conditions. From this point of view, gas foaming (GF) with physical blowing agent such as carbon dioxide, nitrogen or their mixtures has attracted large interest in the past few years [9–11]. Indeed, this technique allows a fine control over the characteristics of the porous network of the scaffold, and avoids the use of organic solvents that may damage transplanted cells and nearby tissues or inactivate the biological signals eventually incorporated into the matrix [9]. Unfortunately, the preparation of gas-foamed scaffolds characterized by 100% open porosity is often impaired by a combination of rheological and processing limitations that hinder the complete pore opening during foaming and lead to the formation of a closed external skin [9,10].

One of the most efficient strategy to overcome these limitations has been found to be the dispersion of a second phase (opening phase) into the polymeric matrix [12,13]. This opening phase is characterized by different deformation behavior with respect to the matrix and, during foaming, may allow for the occurrence of mechanisms of pore opening, therefore increasing the final open-pore content up to 100% [12,13]. By the way, the presence of the residual opening phase into the scaffold may represent an important drawback if this material is not biocompatible. Conversely, the use of an opening phase that may be subsequently removed from the foam may be preferable, acting also as templating phase and allowing the formation of additional open porosity into the inner and outer regions of the scaffold [14].

In this study, two different templating agents, NaCl microparticles and thermoplastic gelatin (TG), have been used for the preparation of gas-foamed poly(ε-caprolactone) (PCL) scaffolds with well-controlled porous networks and high degree of open porosities. The effect of the nature and concentration of the opening phase on the microstructural properties of the foams has been evaluated before and after the reverse templating process. The results demonstrated that by the proper selection of the templating agent and GF process parameters is has been possible the design of foamed structures suitable to be used as scaffolds for specific biomedical applications.

EXPERIMENTAL PART

Materials

PCL ($M_W = 65$ kDa, $T_M = 59$–64°C and $\rho_{PCL} = 1.145$ g/cm^3) and gelatin powder (type B, $M_W = 40$–50 kDa) were purchased from Sigma-Aldrich (Italy). Anhydrous glycerol with purity grade higher than 99.5% was

Downloaded from http://cel.sagepub.com at Matematica Applicata E on February 19, 2009

purchased by Fluka (Italy) and used as plasticizer for the preparation of TG.

NaCl particles (J.T. Beker, Italy) with two different crystal size dimensions (mean particles diameter 5 μm ca. and mean particles diameter in the 300–500 μm range) were used for microparticulate templating (MT) opening phase. The 5μm microparticles were obtained by milling the NaCl in an Ultra-Centrifugal mill (Z100, RETSCH, Italy) equipped with a 80 μm grind size at milling speed of 14.000 rpm.

N_2 and CO_2 mixtures (Air liquide, Italy) were used as physical blowing agents for GF experiments.

Methods

As schematically illustrated in Figure 1, the GF–reverse templating process is a three-step process: (1) preparation of the PCL–NaCl composites or PCL–TG co-continuous blend by melt mixing process, (2) GF of the heterogeneous system with N_2–CO_2 mixtures, and (3) selective extraction of the templating agents.

Mixing

PCL–NaCl composites with compositions in the range 30–70 to 10–90 wt% were prepared by using an internal mixer (Rheomix® 600,

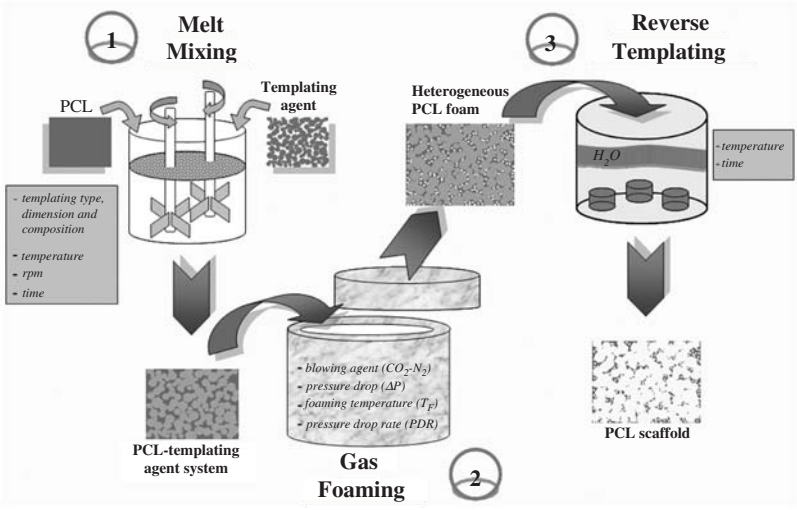

Figure 1. Scheme of the GF–reverse templating three-step process.

Downloaded from http://cel.sagepub.com at Matematica Applicata E on February 19, 2009

Haake, Germany) controlled by a measuring drive unit (Rheocord® 9000, Haake, Germany). PCL pellets were first brought to molten state, and subsequently, NaCl particles were added into the mixing chamber and mixed with the polymer at 70°C, 100 rpm for 10 min, for the milled particles (5 μm), and at 140°C, 20 rpm for 10 min for the 300–500 μm ones. Finally, the composites were extracted from the mixer and compressed into 3 mm thick plates by a hot press (P 300 P, Collin, Germany) at the same temperature of mixing and at 30 bar.

PCL–TG co-continuous blends were prepared as described in a previously reported work [15]. Briefly, TG was prepared by melt mixing 50 g of gelatin powder with 20 wt% of glycerol at 60°C, 60 rpm for 6 min, in the same mixing equipment used for the preparation of the composites. Subsequently, the PCL–TG co-continuous blends were prepared by mixing the two polymers at 60°C, 80 rpm for 6 min in a composition range of 60–40 to 40–60 wt% Finally, the blends were compressed at 70°C and 30 bar into 3 mm thick plates.

Foaming

Disc-shaped samples ($d = 10$ mm, $h = 3$ mm) were saturated with N_2–CO_2 blowing mixtures (0–100 to 80–20 vol%) in a high-pressure vessel (HiP, Pennsylvania, USA) [16], at a saturation pressure (P_{sat}) ranging from 65 to 180 bar and at a saturation temperature (T_{sat}) of 70°C for 4 h. After the blowing agent solubilization, the samples were cooled to the desired foaming temperature (T_F) with a precise cooling profile. The pressure was then quenched to ambient pressure with controlled pressure drop rates. The GF processing variables were the N_2–CO_2 vol% of the blowing agent and T_F. The foams were finally soaked in stirred distilled H_2O at room temperature, for the PCL–NaCl–foamed composites, and at 38°C for the PCL–TG foamed blend, until constant weight was achieved and subsequently vacuum dried. The time required for the complete templating agent extraction varied from 7 days for the PCL/TG-foamed blends to 40 days for the PCL/NaCl composites with milled particles.

Characterization

The microstructure of the foamed samples was analyzed by scanning electron microscopy (SEM). The foams were cross-sectioned, gold sputtered and analyzed by SEM (S440, LEICA, Germany), and the mean cell diameter (D_C) was evaluated by image analysis, according to the ASTM D3576.

Downloaded from http://cel.sagepub.com at Matematica Applicata E on February 19, 2009

The porosity of the scaffolds was determined from the mass and the volume of each foamed sample by using the following equation:

$$\% \text{ porosity} = \left[1 - \left(\frac{\rho_{\text{FOAM}}}{\rho_{\text{PCL}}}\right)\right] \times 100 \quad (1)$$

where ρ_{FOAM} is the apparent density of the foam calculated from mass and volume measurements. The mass was measured by using an high accuracy balance (10^{-3} g, AB104-S, Mettler Toledo, Italy) while the volume determined by displacement method for the scaffolds prepared by using the milled NaCl, or by geometrical calculation, for the scaffolds prepared by the others templating agents, namely the 300–500 μm NaCl and TG.

Image analysis (Image J®) was also used to assess the pore volume and the volume fraction of the two different scaled porosities by means of the area fraction measurements [15]. In particular, the area fraction of the TG-foamed phase or the NaCl porosity provided the macroporosity volume fraction, while the difference between the overall porosity and the macroporosity amount allowed the evaluation of the microporosity volume fraction.

The effect of the scaffold microstructure on the compressive mechanical properties was evaluated by testing the same samples used for porosity calculation. Five cylindrical samples for each scaffold type were tested on an Instron 4204 (Instron, Italy) at a cross head of 1 mm/min and with a 1 kN loading cell. The elastic compressive modulus was determined as the slope of the initial linear portion of the stress versus strain curve.

RESULTS

The microarchitecture of the scaffolds that can be achieved with the GF and reverse templating combined technique strongly depends on several factors, related to the materials and the processes involved. In particular, the nature and concentration of the templating agent and the processing parameters have a key role in defining the final microstructural properties of the scaffold. Moreover, all of these processes are mutually correlated and interdependent. For instance, the amount of the templating agent affects GF, but also defines the additional porosity that can be obtained by the reverse templating step.

In this study, we investigated the effect of the different templating agents and GF processing variables on the morphology of the foams

Downloaded from http://cel.sagepub.com at Matematica Applicata E on February 19, 2009

before and after the selective extraction step, and we described the microstructural features of selected scaffolds, which are more interesting for biomedical applications. We will first report on structures obtained via GF of PCL–NaCl and PCL–TG heterogeneous systems, and then on the structures obtained via the removal of the templating agents.

GF of Heterogeneous Systems

This section describes two examples of the results of the GF process on the heterogeneous systems, to evidence some of the most important peculiarities of the two different templating agents. The analysis of the whole range of effects of the different processing variables (coupled with the effect of formulation) is too complex and is beyond the scope of the present study.

In Figure 2 are reported the morphologies of the foams prepared starting from (a) PCL–NaCl microparticulate composite with 30 wt% of milled NaCl (5 μm), and (b) 60–40 wt% PCL–TG co-continuous blend (the selected GF parameters are reported in the figure caption).

As evidenced in the SEM micrograph of Figure 2(a), the foamed composite is characterized by an interconnected porosity, with the presence of the NaCl microparticles on the pore walls, and also at the pore interconnections (white arrows). In effect, the NaCl microparticles (hard domains) may possibly act as de-bonding sites for the pore walls (soft domains), due to the different deformation behavior between the inorganic and organic phases, thereby promoting the pore opening during foaming [12,13,17]. Furthermore, the presence of the inorganic

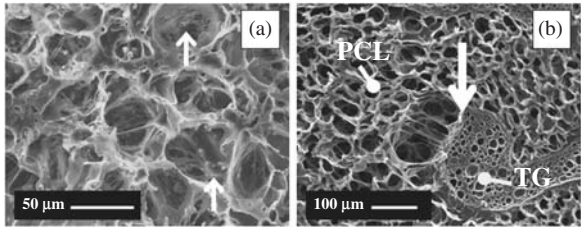

Figure 2. SEM micrographs of the foamed systems before the templating extraction: (a) 70–30 wt% PCL–NaCl composite foamed with CO_2 at $T_F = 32^\circ C$, $P_{sat} = 65$ bar, and PDR = 200 bar/s; (b) 60–40 wt% PCL–TG co-continuous blend foamed with 80–20 vol% N_2–CO_2 blowing mixture at $T_F = 44^\circ C$, $P_{sat} = 180$ bar, and PDR = 700 bar/s. The arrows indicate (a) the NaCl microparticles located on the pore walls and at the pore interconnection; (b) the interface between the foamed PCL and TG phases.

Downloaded from http://cel.sagepub.com at Matematica Applicata E on February 19, 2009

filler into the polymeric matrix enhances the pore walls stiffness and limits the open-pore coalescence [12,13,17].

SEM of the PCL–TG foamed sample (Figure 2(b)), conversely, shows a morphology characterized by two foamed phases, with PCL-foamed phase characterized by bigger and highly opened pores with respect to the tiny and closed pore of the TG phase. This effect may be explained by considering that the glass transition temperature of the TG is close to 40°C [18] (about 100°C higher than that of the PCL). At $T_F = 44$°C, consequently, the viscosity of the TG domains is too high to produce high expansion ratios. Moreover, as evidenced in the SEM micrograph, the interface between the PCL and TG phases may act as site for preferential nucleation and opening of the pores created into the PCL phase (see arrow in Figure 2(b)) [12,13,15].

GF–microparticulate Templating Scaffolds

In Figure 3 are reported the SEM micrographs of the scaffolds prepared from 10–90 wt% PCL–NaCl composite, by using 300–500 μm templating particles, before (Figures 3(a) and (c), lower and higher magnification) and after (Figures 3(b) and (d), lower and

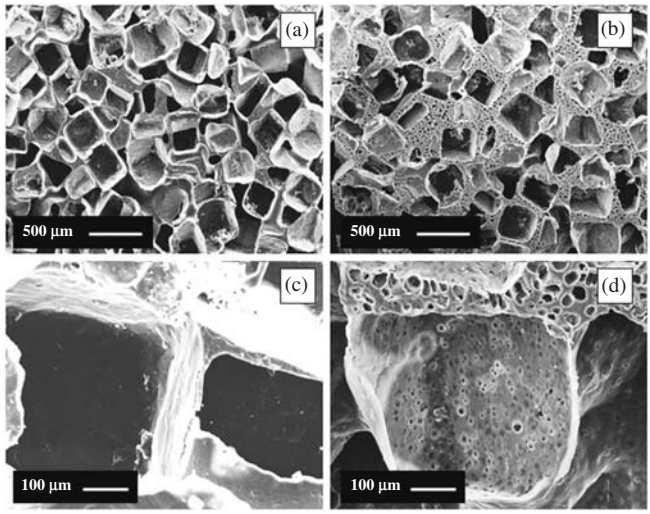

Figure 3. SEM micrographs of the PCL scaffold before and after the foaming process: (a and c) 10–90 PCL–NaCl (300–500 μm) wt% MT scaffold; (b and d) 10–90 PCL–NaCl (300–500 μm) wt% GF/MT scaffold foamed with 60–40 vol% N_2–CO_2 blowing mixture at $T_F = 35$°C, $P_{sat} = 150$ bar, and PDR = 500 bar/s.

Downloaded from http://cel.sagepub.com at Matematica Applicata E on February 19, 2009

higher magnification) the GF process (details of GF experiments are reported in the figure caption). As evidenced in the lower magnification of Figures 3(a) and (b), both the scaffolds are characterized by cubic-shaped pores created after NaCl leaching. However, the presence of additional rounded pores induced by GF is evident in Figure 3(b). In effect, as evidenced in Figure 3(c) (higher magnification of the non-foamed scaffold reported in Figure 3(a)), the scaffold prepared by the NaCl MT showed a porous structure with almost intact pore walls, proving very limited contact points between adjacent crystals in the polymer network [19]. Indeed, by combining GF and MT, pores of 40 μm diameter are created on the walls of the pores obtained by NaCl leaching (Figure 3d).

These results have been confirmed by the porosity distribution measurements reported in Table 1. Indeed, even if the MT and the GF/MT scaffolds were characterized by similar overall porosity amounts, changes in the pore size distribution were observed. In particular, for the GF/MT scaffolds, we observed 90% ca. of pores with mean pore size of the order of hundred of microns (macroporosity), created by the removal of the NaCl. Furthermore, the 10% ca. remaining was formed during GF of PCL and characterized by mean pore size of 36 μm (microporosity).

Totally different morphologies may be achieved by using smaller NaCl microparticles for the preparation of the scaffold. In particular, Figure 4 reports the micrographs of the foams prepared by GF/MT and by using 5 μm NaCl particles. In this case, the MT agent acts as a micrometric filler dispersed into the polymeric matrix, affecting its viscoelastic properties and foaming behavior [17,20,21]. Again, by controlling the T_F and the concentration of the microparticulate porogen, it was possible to fine tune the microarchitecture of the scaffold (see Figure 4 and corresponding caption for the experimental details). In particular, the increase of the T_F

Table 1. Porosity distribution of different scaffolds prepared.

	MT	GF/MT	GF/PT
Overall porosity (%)	82 ± 0.7	83.2	62
Macroporosity			
Percentage	100	89.5	44
Mean pore size (μm)	336 ± 97	307 ± 118	312 ± 77
Microporosity			
Percentage	/	10.5	56
Mean pore size (μm)	/	36.6 ± 8.9	38.05 ± 11

Downloaded from http://cel.sagepub.com at Matematica Applicata E on February 19, 2009

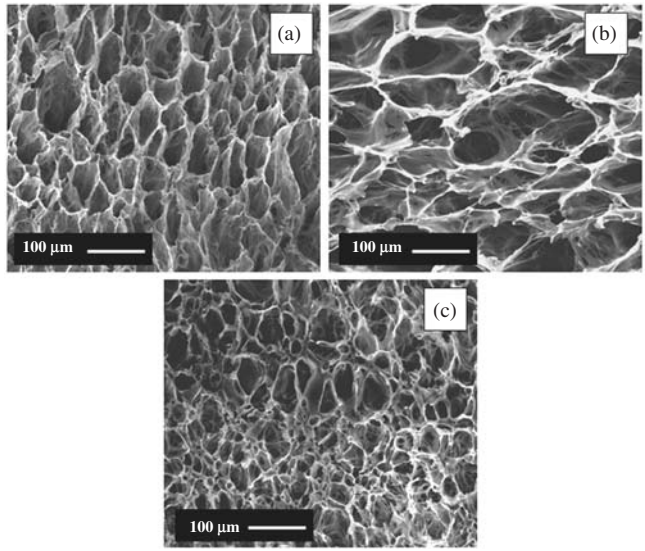

Figure 4. SEM micrographs of the PCL scaffold prepared by GF/MT with 5 μm NaCl particles: 70–30 wt% PCL–NaCl composite foamed with CO_2 at $P_{sat} = 65$ bar, PDR = 200 bar/s and (a) $T_F = 25°C$, (b) $T_F = 28°C$; (c) PCL scaffold with spatial gradient of porosity and pore size prepared with 40/60 NaCl spatial concentration and foamed with CO_2 at $T_F = 32°C$, $P_{sat} = 65$ bar, and PDR = 200 bar/s.

from 25°C to 28°C (Figures 4(a) and (b), respectively), resulted in the decrease of the viscosity of the matrix and the corresponding achievement of scaffolds with a higher degree of open porosity (up to 92%) and interconnectivity. Furthermore, as reported in Figure 4(c), scaffold with anisotropic architecture may be prepared by creating spatial gradient of NaCl concentration [17]. In particular, the region of the sample with 40 wt% microparticles concentration, (upper zone of SEM micrograph reported in Figures 4c) showed higher porosity and pore size (88% and 58 μm, respectively) with respect to that with 60 wt% of NaCl (lower zone, 83% and 24 μm, respectively).

GF/polymer Templating Scaffolds

SEM micrographs of the scaffold prepared by the GF/polymer templating (PT), after the selective extraction of the TG from the foamed blend described previously in Figure 2(b), are reported in Figure 5.

Downloaded from http://cel.sagepub.com at Matematica Applicata E on February 19, 2009

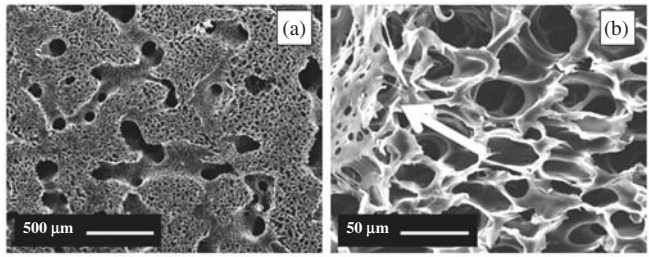

Figure 5. SEM micrographs of multiscaled PCL scaffold prepared by GF/PT from 60–40 PCL–TG co-continuous blend, solubilized with 80–20 vol% N_2–CO_2 blowing mixture at $P_{sat} = 180$ bar and foamed at $T_F = 44^{\circ}C$ and PDR = 700 bar/s: (a) lower magnification of scaffold microstructure; (b) details of the microporosity and the interface between micro- and macroporosity (white arrow).

As expected, the lower magnification of Figure 5(a) reveals that, by this technique, it was possible to prepare scaffolds with pore size and shape on a double scale: a macroporosity created by the removal of the TG foamed phase and a microporosity (mean pore size of 38 μm, Table 1), formed during GF of PCL. In particular, the macroporosity appears elongated, interconnected, and homogeneously distributed around the interconnected and circular-shaped microporosity (see the higher magnification of Figure 5(b)). Furthermore, the interface between the two different scaled porosities (white arrow in Figure 5(b)) is characterized by the presence of an additional interconnectivity, probably induced by the preferential nucleation and opening of the pores at the interface between the two polymeric phases (see also, for comparison, Figure 2(b), white arrow).

DISCUSSION

As extensively described in literature, the GF allows a fine control over the characteristics of the porous network of the scaffold by the selection of the proper operating conditions [9–11], while, with the addition and subsequently removing of the templating agent, the scaffold microstructure can be further tuned by modifying the templating type and concentration, giving an additional degree of freedom in the design of the porous network.

It has to be underlined, however, that the addition of templating agents to the PCL strongly influences its foaming behavior: several factors, such as templating nature, size, shape, and concentration, have a strong influence on the viscoelastic properties of the heterogeneous systems, on the nucleation and growth of gas bubbles, on the

Downloaded from http://cel.sagepub.com at Matematica Applicata E on February 19, 2009

mechanisms of pore opening during foaming and on the final setting of the porous network of the scaffold.

By the selection of 300–500 μm NaCl microparticles it was possible the preparation of multi-scaled scaffolds characterized by bimodal pore size and shape and enhanced interconnectivity with respect to those prepared by the NaCl templating alone. In effect, the MT without subsequent GF does not allow the achievement of sufficient pore interconnectivity because of the limited contact among the microparticles (Figure 3(a) and (c)). The resulting cellular structure would significantly hinder both the cell penetration into the inner part of the scaffold and the transport of nutrients and metabolic wastes necessary to support the cell viability, and to prevent the development of a necrotic tissue into the interior of the scaffold [5,8]. The porosity created by the GF, conversely, may assure the formation of an additional interconnection among the macroporous walls, overcoming the lack of pore interconnection of the scaffold prepared by the MT alone (Figure 3(b) and (d)).

The reduction of NaCl dimension (from 300–500 μm to 5 μm) significantly modified the foaming behavior of the PCL (compare Figures 3 and 4). In particular, NaCl particles dispersed into the polymeric matrix modify its flow behavior and foamability properties, as already discussed [17]. Moreover, the NaCl particles have a great impact on the mechanism of pore opening during foaming because of the concurrent de-bonding and strengthening effects, and for the additional interconnectivity produced after leaching (Figure 4(a) and (b)). Furthermore, these characteristics may be tailored with the aim of preparing scaffolds characterized by spatial gradients of porosity and pore size (Figure 4(c)). The possibility of preparing highly interconnected scaffolds with well-controlled anisotropic architectures is strongly required in designing TE scaffold. Indeed, scaffolds characterized by gradients of porosity and pore size offer the great advantage to reproduce the spatial organization of cells and extracellular matrix into highly complex 3D tissues, such as bone and cartilage [6].

It is important to point that it has been possible to complete leach out the NaCl from all the microparticulate foamed systems prepared. However, differences in the NaCl dissolution process may be observed with respect to the different templating size and concentration as well as GF parameters used. Indeed, the penetration of the water into the polymeric matrix, and therefore, the dissolution of the porogen, require the gas outflow from the foamed pores, that was promoted performing the leaching under stirred water. Consequently, for the highly foamed systems, such as those prepared by using the milled NaCl particles, longer

Downloaded from http://cel.sagepub.com at Matematica Applicata E on February 19, 2009

soaking time are required to achieve the complete extraction of the porogen, if compared to the 300–500 μm NaCl particles foamed composites (as pointed in the Methods section).

One of the most important limitation of the scaffolds prepared by using MT-based techniques is related to the low capability to sustain the mechanical loading during *in vivo* TE applications. In fact, to achieve a high degree of interconnectivity there is a need of high expansion ratios or templating concentration. As a consequence, these scaffolds are characterized by high degree of overall porosity, often higher than 80% (Table 1), with the consequent detriment of the mechanical properties. From this point of view, the use of PT technique offers the great advantage to prepare scaffolds characterized by a lower overall porosity (62% for the scaffold reported in Figure 5, Table 1), with highly interconnected porosity. As a direct consequence, this scaffold is characterized by enhanced mechanical properties with respect to those prepared with the MT alone. Figure 6 reports the stress versus strain curves obtained by static compression test performed on the scaffolds reported in Figures 3 and 5. It can be observed that, the scaffold prepared with the MT based techniques (MT and GF/MT) evidenced the typical stress versus strain curve of low density cellular materials, characterized by a linear-elastic region followed by a plateau of roughly constant stress leading into a final region of steeply rising stress [22]. The GF/PT scaffold, conversely, had higher stress values in all of the deformation range evaluated, with no evidence of the plateau region. The enhanced mechanical properties of this scaffold is also confirmed by an increase of almost one order of magnitude in the elastic compressive

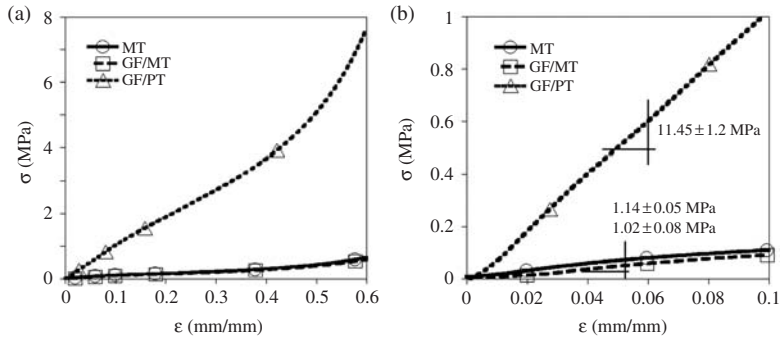

Figure 6. (a) Stress vs. strain curves obtained by static compressive tests of the scaffolds prepared: MT and GF/MT scaffolds of Figure 3; GF/PT scaffold of Figure 5; (b) elastic regions of the stress versus strain curves of the scaffolds and correspondent elastic compressive moduli.

Downloaded from http://cel.sagepub.com at Matematica Applicata E on February 19, 2009

modulus (11.45 MPa), as evidenced in Figure 6(b). In view of the regeneration of load-bearing tissues, such as bone and cartilage, the GT/PT resulted the best combination to achieve scaffold with optimal pore size and interconnectivity and mechanical properties.

CONCLUSIONS

Scaffold design is becoming one of the most efficient strategy in TE to guide the regeneration of functional biological tissues.

In this work, we investigated the possibility of fine tune the microstructural properties of PCL scaffolds by combining GF and reverse templating techniques. In particular, the effect of the templating agent nature, size, shape, and concentration on the foaming of PCL was surveyed, and the GF process parameters optimized with the aim of fine control the microstructural properties of the scaffolds.

The opportune selection of the polymer and templating agent and GF process parameters allowed the preparation of highly interconnected PCL scaffolds with different porosity, pore size and interconnectivity, and multiscaled porous architectures.

REFERENCES

1. Hutmacher, D.W. (2000). Scaffolds in Tissue Engineering Bone and Cartilage, *Biomaterials*, **21**: 2529–2543.
2. Kim, B. and Mooney, D.J. (1998). Development of Biocompatible Synthetic Extracellular Matrices for Tissue Engineering, *TIBTECH*, **16**: 224–230.
3. Yang, S., Leong, K., Du, Z. and Chua, C. (2001). The Design of Scaffolds for Use in Tissue Engineering. Part I. Traditional Factors, *Tissue Engineering*, **7**(6): 679–689.
4. Zeltinger, J., Sherwood, J.K., Graham, D.A., Müeller, R. and Griffith, L.G. (2001). Effect of Pore Size and Void Fraction on Cellular Adhesion, Proliferation, and Matrix Deposition, *Tissue Engineering*, **7**: 557–572.
5. Moore, M.J., Jabbari, E., Ritman, E.L., Lu, L., Currier, B.L., Windebank, A.J. and Yaszemski M.J. (2004). Quantitative Analysis of Interconnectivity of Porous Biodegradable Scaffolds with Micro-computed Tomography, *Journal of Biomedical Material Research*, **71A**: 258–267.
6. Woodfield, T.B.F., Van Blitterswijk, C.A., De Wijn, J., Sims, T.J., Hollander, A.P. and Riesle, J. (2005). Polymer Scaffolds Fabricated with Pore-Size Gradients as a Model for Studying the Zonal Organization within Tissue-Engineered Cartilage Constructs, *Tissue Engineering*, **11**: 1297–1311.
7. Lin-Gibson, S., Cooper, J.A., Landis, F.A. and Cicerone, M.T. (2007). Systematic Investigation of Porogen Size and Content on Scaffold Morphometric Parameters and Properties, *Biomacromolecules*, **8**: 1511–1518.

Downloaded from http://cel.sagepub.com at Matematica Applicata E on February 19, 2009

8. Karande, T.S., Ong, J.L. and Agrawal, C.M. (2004). Diffusion in Musculoskeletal Tissue Engineering Scaffolds: Design Issues Related to Porosity, Permeability, Architecture, and Nutrient Mixing, *Annals of Biomedical Engineering*, **32**(12): 1728–1743.
9. Mooney, D.J., Baldwin, D.F., Suh, N.P., Vacanti, J.P. and Langer, R. (1996). Novel Approach to Fabricate Porous Sponges of poly(D,L-lactic-co-glycolic acid) Without the Use of Organic Solvents, *Biomaterials*, **17**: 1417–1422.
10. Barry, J.J.A., Gidda, H.S., Scotchford, C.A. and Howdle, S.M. (2004). Porous Methacrylate Scaffolds: Supercritical Fluid Fabrication and *In Vitro* Chondrocyte Responses, *Biomaterials*, **25**: 3559–3568.
11. Mathieu, L.M., Mueller, T.L., Bourban, P., Pioletti, D.P., Muëller, R. and Månson, J.E. (2006). Architecture and Properties of Anisotropic Polymer Composite Scaffolds for Bone Tissue Engineering, *Biomaterials*, **27**: 905–916.
12. Lee, P.C., Wang, J. and Park, C.B. (2006). Extruded Open-cell Foams Using Two Semi-crystalline Polymers with Different Crystallization Temperatures, *Industrial & Engineering Chemistry Research*, **45**: 175–181.
13. Lee, P.C., Wang, J. and Park, C.B. (2006). Extrusion of Microcellular Open-Cell LDPE-Based Sheet Foams, *Journal of Applied Polymer Science*, **102**: 3376–3384.
14. Harris, D.L., Kim, B. and Mooney, D.J. (1998). Open Pore Biodegradable Matrices Formed with Gas Foaming, *Journal of Biomedical Material Research*, **42**: 396–402.
15. Salerno, A., Oliviero, M., Di Maio, E., Iannace, S. and Netti, P.A. (2007). Design and Preparation of μ-Bimodal Porous Scaffold for Tissue Engineering, *Journal of Applied Polymer Science*, **106**: 3335–3342.
16. Marrazzo, C., Di Maio, E., Iannace, S. and Nicolais, L. (2008). Process-Structure Relationships in PCL Foaming, *Journal of Cellular Plastics*, **44**(1): 37–52.
17. Salerno, A., Iannace, S. and Netti, P.A. (2008). Open-Pore Biodegradable Foams Prepared via Gas Foaming and Microparticulate Templating. *Macromolecular Bioscience*, **8**: 655–64.
18. Salerno, A., Oliviero, M., Di Maio, E. and Iannace, S. (2007). Thermoplastic Foams from Zein and Gelatin, *International Polymer Processing*, **5**: 480–488.
19. Zhang, J., Wu, L., Jing, D. and Ding, J. (2005). A Comparative Study of Porous Scaffolds with Cubic and Spherical Macropores, *Polymer*, **46**: 4979–4985.
20. Hornsby, P.R. (1999). Rheology, Compounding and Processing of Filled Thermoplastics, *Advances in Polymer Science*, **139**: 155–217.
21. Teng, X., Ren, J. and Gu, S. (2007). Preparation and Characterization of Porous PDLLA/HA Composite Foams by Supercritical Carbon Dioxide Technology, *Journal of Biomedical Material Research Part B*: *Applied Biomaterials*, **81B**: 185–193.
22. Kweon, H., Yoo, M.K., Park, I.K., Kim, T.H., Lee, H.C., Lee, H., Oh, J., Akaike, T. and Cho, C. (2003). A Novel Degradable Polycaprolactone Networks for Tissue Engineering, *Biomaterials*, **24**: 801–808.

Downloaded from http://cel.sagepub.com at Matematica Applicata E on February 19, 2009